Molecular & Biochemical Parasitology 211 (2017) 9–14

Contents lists available at ScienceDirect

Molecular & Biochemical Parasitology

Proteomic investigation of human cystic echinococcosis in the liver

Rémi Longuespée[a,b,*], Rita Casadonte[a], Mark Kriegsmann[b], Petra Wandernoth[c], Katharina Lisenko[d], Gabriel Mazzucchelli[e], Michael Becker[f], Jörg Kriegsmann[a,c,g]

[a] Proteopath GmbH, Trier, Max Planck Strasse 17, 54296 Trier, Germany
[b] Institute of Pathology, University of Heidelberg, Im Neuenheimer Feld 224, 69120 Heidelberg, Germany
[c] Molecular Pathology Trier, Max Planck Strasse 17, 54296 Trier, Germany
[d] Department of Internal Medicine V, University of Heidelberg, Im Neuenheimer Feld 410, 69120 Heidelberg, Germany
[e] Mass Spectrometry Laboratory (LSM), Systems Biology and Chemical Biology, GIGA-Research, University of Liège, Allée du 6 aoÛt 11, 4000 Liège, Belgium
[f] Bruker Daltonik GmbH, Bremen, Germany, Fahrenheitstrasse, 28359 Bremen, Germany
[g] MVZ for Histology, Cytology and Molecular Diagnostics Trier, Max Planck Strasse 5, 54296 Trier, Germany

ARTICLE INFO

Article history:
Received 4 October 2016
Received in revised form
21 November 2016
Accepted 9 December 2016
Available online 13 December 2016

Keywords:
Histoproteomics
Cystic echinococcosis
Laser microdissection
Parasitic disease
MALDI IMS

ABSTRACT

Cystic echinococcosis (CE) is a pandemic infectious disease caused by the tapeworm *Echinococcus granulosus* that forms cysts in different organs such as lungs and liver. Imaging examination and serological tests have some drawbacks such as low sensitivity. In this study, we used an up-to-date workflow of laser microdissection-based microproteomics and matrix-assisted laser desorption/ionization time-of-flight imaging mass spectrometry in order to depict the proteomic pattern of CE in the liver. This investigation revealed specific markers of a parasitic cyst in liver. This proteomic pattern could facilitate diagnosis of CE in the future.

1. Introduction

Cystic echinococcosis (CE) is an endemic parasitic disease which is caused by infection with metacestodes (larval stage) of the tapeworm *Echinococcus granulosus* (Eg) [1]. Humans as well as herbivores such as sheeps, goats or cattle are accidental intermediate hosts that become infected by ingested water, food, or soil contaminated with faeces from infected carnivores such as dogs or foxes which are definite hosts. Upon ingestion of the eggs, oncopheres are released that have the capacity to penetrate the human intestinal wall where they gain access to the portal venous system and subsequently various organs where the oncospheres develop into cysts. The liver (70%) and lungs (20%) are most commonly affected. However, cyst formation can occur anywhere in the body (10%). Since the clinical course is relatively quiescent and patients present with mild symptoms that are dependent on the cyst location and size, CE poses challenges for accurate and timely diagnosis. Additionally it can be expected that increased emigration of populations where prevalence rates are as high as 5–10% such as in certain parts of South Africa, Eastern Europe, Russia, the Middle East, and China raise the possibility to attend patients affected by CE also in western countries [2]. Diagnosis is usually achieved by a combination of clinical history, serum analyses and imaging observation such as ultrasound, computed tomography or magnetic resonance tomography. Whereas in early infections, serological studies are used, in late stages imaging studies are usually performed [3]. Although the host does produce detectable humoral and cellular responses, serological studies suffer from low sensitivities ranging from 30 to 80% depending on the assay employed [4]. In some cases the diagnosis of CE is delayed until histopathological examination of the resection specimen, especially in uncommon locations of echinococcal cysts for example ossal, intramuscular, retroperitoneal or spinal [5–9]. To confirm the diagnosis of CE a Periodic acid Schiff (PAS)

Abbreviations: ACN, Acetronitrile; CA, Citric acid; CE, Cystic echinococcosis; Eg, *Echinococcus granulosus*; ECM, Extra cellular matrix; FFPE, Formalin fixed paraffin embedded; fr/fr, Fresh/frozen; GO, Gene ontology; HIAR, Heat-induced antigen retrieval; HIV, Human immunodeficiency virus; HLA, Human leucocyte antigen; IMS, Imaging mass spectrometry; LMD, Laser microdissection; LC–MS/MS, Liquid chromatography-mass spectrometry/mass spectrometry; MALDI, Matrix-assisted laser desorption-ionization; PAS, Periodic acid Schiff; ID, Protein identification; ROI, Region of interest; TIC, Total ion count; UPLC, Ultra-performance liquid chromatography.

* Corresponding author at: Im Neuenheimer Feld 224, 69120 Heidelberg, Germany.
E-mail address: remi.longuespee@med.uni-heidelberg.de (R. Longuespée).

http://dx.doi.org/10.1016/j.molbiopara.2016.12.002
0166-6851/

reaction is routinely performed since the tapeworm stains PAS-positive. Treatment mostly relies on surgery for the removal of the cysts and chemotherapy [1].

CE has been studied on the genetic level previously [10,11]. Even though proteomic investigations have been performed in the past [12–20], few of new protein sequences of Eg have been reported in databases. The proteome of Eg is indeed still poorly described in universal databases such as Uniprot, with only few protein sequences available. Moreover, very few studies have been executed on human samples.

In the present study, we applied up-to-date methods for the proteomic analysis of formalin-fixed and paraffin-embedded (FFPE) tissues, the standard processing method to store tissues in pathology institutes worldwide.

We used laser microdissection (LMD)-based liquid chromatography tandem mass spectrometry (LC–MS/MS) for the simultaneous extraction and digestion of proteins from specific tissue regions in a patient with CE: the cyst liquid containing the worm, the cystic wall and the surrounding liver tissue. Additionally, we performed matrix-assisted laser desorption/ionization time-of-flight (MALDI) imaging mass spectrometry (IMS) to correlate proteomic data and morphology. This is the first study to perform LMD and IMS on FFPE tissue from a patient with CE and, to the best of our knowledge, the first report combining LMD and IMS for the diagnosis of CE.

2. Material and methods

2.1. Preanalytics

The tissue sample was provided by the University of Heidelberg with institutional ethical review approval. After surgery, the tissue was fixed in buffered formalin, embedded in paraffin, and sectioned [21]. PAS reaction was performed for the visualization of polysaccharides, glycogen, glycoproteins and glycolipids in the tissue section.

Materials for LMD analyses and IMS were described previously [21,22].

2.2. LMD and LC–MS/MS

Different regions of interest (ROIs) of the tissue section, including the cyst fluid containing Eg (“cyst” in the article), the cystic wall and the surrounding liver tissue (“liver” in the article) were collected in three different tubes (Fig. 1**, panel A).**

LMD was used as a sampling method for this investigation as it appeared to be the best one for the accurate selection of the different parts composing the tissue. The tissues were processed following a procedure that avoids tissue loss during biochemical preparation [21]. This method was specifically designed for FFPE tissues. This relies on the biochemical processing including the proteolytic digestion of fixed proteins directly from the laser microdissected tissue piece, in a tube.

Peptides were subsequently separated by reverse-phase LC using ultra performance liquid chromatography (UPLC) 2D nanoAcquity (Waters, Corp., Milford, USA), and analyzed using a Thermo Scientific Q Exactive Hybrid Quadrupole-Orbitrap mass spectrometer (Thermo Fisher Scientific, Waltham, USA) [21]. A first step of one dimension LC–MS/MS analysis with a 180 min run with 200 ms of accumulation of MS peaks for further MS/MS, and the selection of 10 of the major MS peaks for MS/MS, was performed to estimate the quantity of the peptide content in each sample. 2D LC–MS/MS analyses (RP x RP, high and low pH) included three isocratic elution steps on which 180 min LC gradient were performed, as described before [21]. The time for accumulation of MS peaks for further MS/MS was 200 ms 10 of the major MS peaks were selected for MS/MS.

2.3. Data processing

MaxQuant version 1.5.2.8 was used for protein identifications (IDs) from raw files. MS/MS spectra were analyzed to retrieve peptide sequences and to compare those to databanks, for identification. Andromeda search engine with the Uniprot database from *Homo sapiens* and Eg (released versions 2015-04) was used for interrogation. The following modifications were set for identification: N-ter acetylation, oxidation of methionines, deamidation as variable modifications, carbamidomethylation of the cysteines as fixed modification. The maximum number of missed cleavages was set at seven amino acids. At least two peptides per protein, including one unique peptide were required for identification.

A Venn diagram was made from the list of the proteins identified in each of the samples in order to differentiate the ones that are common between different ROIs and the ones that are only found in a specific ROI [23]. The Uniprot entry of the proteins identified in each compartment were listed in the “GeneVenn” website (http://genevenn.sourceforge.net/). Since three lists can be inserted, a Venn diagram containing the number of proteins commonly found in the different compartments of interest in the liver infected by Eg could be obtained. The Venn diagram was then manually reconstructed in order to adapt the size of the overlapping cells proportionally to the number of proteins.

Gene ontology (GO) annotation of the proteins specifically found in the different tissue parts was performed using Blast2GO 3.2. For each compartment of the infected liver tissue, a FASTA file listing the identified proteins was created. Each of the sequences was blasted against sequences of the Swissprot database, using the National Center for Biotechnology Information (NCBI) Blast service. The blasted sequences were then mapped in order to link the protein IDs to the GO database. The GO database contains millions of functionally annotated gene products for hundreds of species. The molecular function, biological process and cellular component were retrieved from the GO database. Level 3 GO were selected for representation. The number of sequences that were assigned to each GO was reported, and the nine most represented GO were used to create a histogram.

Since two species were checked for the analysis, no filter for taxonomy was applied.

2.4. IMS

FFPE tissue section was subjected to *in situ* trypsin digestion, sprayed with α-Cyano-4-hydroxycinnamic acid matrix for IMS analysis as described before [22,24] and analyzed using a rapifleX MALDI Tissuetyper mass spectrometer (Bruker, Bremen, Germany), with data acquired at 50 μm spatial resolution. IMS dataset was imported into SCiLS Lab (SCiLS GmbH, Bremen, Germany) for visualization of images and statistical analysis. 206 monoisotopic peaks from peptides were detected and used for the establishment of the peak list. Total ion count (TIC) normalization was used as well as baseline removal using Top Hat algorithm. Molecular images in Fig. 2 were represented with 50% transparency in order to show tissue regions from the optical image. Hierarchical clustering was chosen for the segmentation process to group the most similar spectra or sets of spectra into clusters.

The identification of the peptides mapped by IMS was made by comparing the masses of the monoisotopic peptides with the one obtained from the LC–MS data. As mainly monocharged peptides were obtained by IMS, the LC–MS values corresponding to [M + H] were used for correlation with IMS values. “M” corresponds to the mass of the peptides reported in the peptide identification table

from the LC–MS analyses, and "H" to the mass of hydrogen. In our experience, H+ species are likely found in FFPE tissues contrary to Na+ or K+ species. The peptides with a mass difference of more than 0.3 Da between IMS and the LC–MS data were discarded from the list of identification candidates.

3. Results

3.1. LMD and LC–MS/MS analyses

Three different compartments were investigated, namely cyst, cyst wall and liver. A total of 2354 IDs were retrieved from these ROI. The IDs were distributed differently between these compartments with 559 in the cyst, 1310 in the cyst wall and 1985 in the normal liver tissue. Overlap between the proteins identified in the various compartments was demonstrated by a Venn diagram (Fig. 1, **panel B**). In each compartment, we found proteins that were not found anywhere else. We found 85 proteins specifically in the cyst, 184 in the cyst wall and 927 in the liver. The list of compartment-specific proteins is reported in **supplementary** Table 1. The name of each of the proteins specifically identified in one compartment of the tissue is provided in the first column of the table. The Uniprot entry of each protein ID is provided in the second column, which gives the information of the species type. The protein IDs are listed by order of abundance, reflected by the intensity reported in column 3.

Additionally, we provided the full list of identified proteins and peptides in **supplementary** Tables 2 **and 3**, respectively.

In **supplementary** Table 2, the protein accession number of the protein groups, the protein names and the corresponding gene names are listed. The number of identified peptides per protein, as well as the number of the unique and razor peptides is depicted. Unique peptides are peptides that are only identified within a protein group. Razor peptides are non-unique peptides assigned to the protein group with the most other peptides. The sequence coverage, sequence length and the molecular weight of the proteins are also given. Finally the intensity values of the proteins indicating their abundance are listed.

In **supplementary** Table 3 all the peptides identified in the cyst, the cyst wall and the liver are listed. The peptides that were correlated to IMS analyses were highlighted in yellow. In this table all the peptide sequences, lengths and masses are shown. The start- and end position are also given, as well as the number of missed cleavages. The gene name and protein name of the corresponding identification are provided. We annotated if the identified peptides were unique or not. It is noteworthy that most of the identified peptides are unique to one protein group. Finally, the intensities of the peptides are given. Since the intensity of a protein is the sum of intensities of peptides, it is important to know the intensities of peptides individually, as the sum of highly intense peptides can result in lower intensity proteins, compared to other proteins containing more peptides but with lower intensity values.

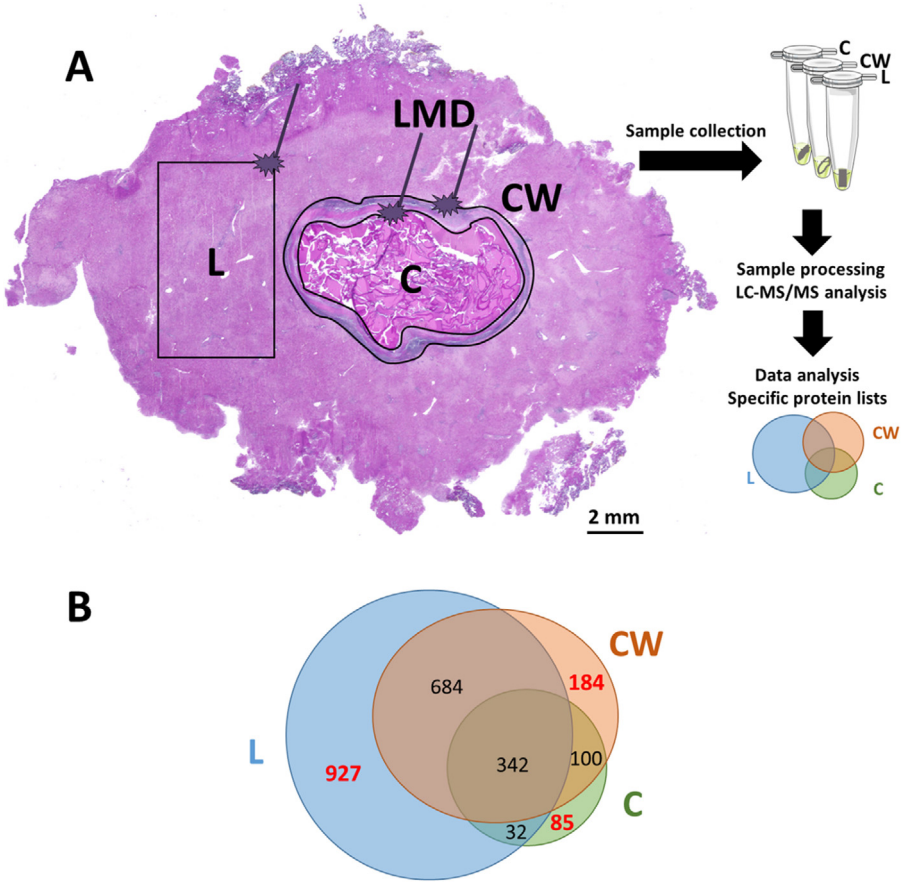

Fig. 1. Laser microdissection-based proteomic workflow for the analysis of a liver infected by *Echinococcus granulosus*. Specific tissue regions of interest (ROI) including the cyst (C), the cyst wall (CW) and the liver (L), were annotated by a pathologist on a Periodic acid Schiff reaction-stained tissue section. The ROIs were then collected by laser microdissection from a serial section. After the biochemical processing, the digested proteolytic peptides were subjected to liquid chromatography-mass spectrometry/mass spectrometry and data analysis (A). A Venn diagram was created from the list of identified proteins in order attribute these proteins to the various tissue compartments (B). We found 85 proteins specifically in the cyst, 184 in the cyst wall, and 927 in the liver. The proteins specifically attributed to one compartment appear in red in the Venn diagram. (For interpretation of the references to colour in this figure legend, the reader is referred to the web version of this article.)

In each of the selected tissues, proteins assigned to both human and Eg species were found. Surprisingly, some proteins assigned to Eg species were only present in the liver and neither in the cyst, nor in the cyst wall. Otherwise, proteins assigned to human species were specifically present in the cyst and/or the cyst wall but not in the liver.

We annotated these specific proteins in function of their GO [25], as described in Section 2.3. The GO database contains the annotation of millions of genes and genes products corresponding to thousands of species, including human and Eg. Three GOs describe a biological compound. The GO "cellular component" describes the subcellular location of the compound of interest at the level of subcellular structures and macromolecular complexes. The GO "molecular function" describes the biochemical ability of a compound. The GO "biological process" describes the series of events resulting from molecular functions of a protein or a group of proteins.

Main GO group child GO that describe most specifically the functionality of the protein. The nine most frequently attributed level 3 GO patterns for cellular component, molecular functions and biological processes were reported in **supplementary** Fig. 1, by order of importance.

Interestingly, in the cyst, antigen binding was the most represented molecular function, and immune functions such as innate immune response proteins were found. Innate immune response, receptor-mediated endocytosis, Fc-receptor-signaling and complement activation pathways were the most frequent biological processes. Among the most intense proteins, different types of immunoglobulin were found, which are all involved in innate immunity. Six out of 85 proteins identified were assigned to Eg species.

In the cyst wall, three out of 184 proteins were assigned to Eg species, namely phospholipase-D1, Ras-related protein Rab–6 B and titin. Many proteins involved in immune response were found in the cyst wall. Among the 30 most intense proteins from the cyst wall, we interestingly found human leucocyte antigen (HLA) histocompatibility antigens class I and II that were not present in the lumen of the cyst. Many extracellular matrix (ECM) proteins such as different collagens, integrins and dermatopontin were found. One of the most intense was tenascin.

The most frequent proteins in the liver were related to physiological biological processes such as oxydoreduction. Furthermore, proteins which belong to nematode larval development and egg hatching have been observed. Even though Eg is a cestode, it shares common biological processes with other parasite worms for its development [26]. Moreover, the Uniprot database lists only 168.503 unreviewed and 61 reviewed protein sequences for the cestodes against 1.235.015 unreviewed and 4690 reviewed proteins for nematodes. Most of the identifications assigned here to nematode larval development may actually be common to cestode larval development.

In the liver, seven out of the 927 proteins specifically found in this tissue were assigned to Eg species.

3.2. Molecular mapping by IMS

A serial tissue section was analyzed by IMS in order to map the peptides in the ROIs: the cyst, the cyst wall and the liver, as presented in Fig. 2. Hierarchical clustering analysis allowed statistical grouping of spectra that were displayed as a spatial segmentation map. This process revealed molecular heterogeneity within the ROIs. The correlation of the IMS data with the LC–MS/MS results allowed us to attribute the identification of some peaks (Fig. 2).

4. Discussion

The identification of the proteome of parasites may facilitate the diagnosis in various tissue compartments. Additionally, scant information is available concerning specific reactions of the surrounding liver tissue to infection by CE. This knowledge may contribute to the development of new therapies against this parasitic infection.

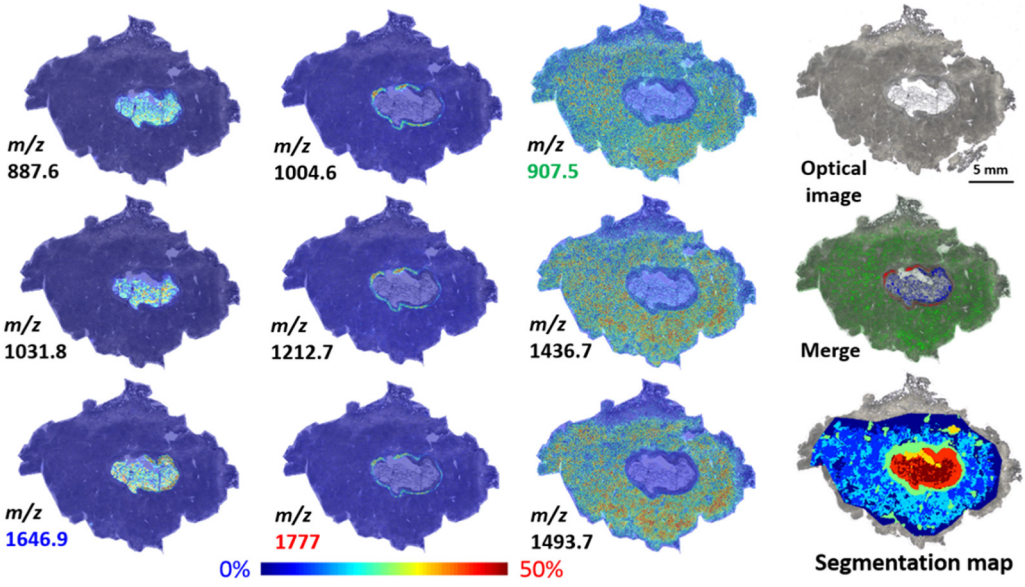

Fig. 2. Matrix-assisted laser desorption ionization imaging mass spectrometry of the liver infected by *Echinococcus granulosus*. The image in the right upper corner is the optical image of the analyzed tissue. Images of several ions specifically present in the regions of interest of the tissue are shown. *m*/*z* values were selected that specifically matched one peptide mass (M + H) from the proteins identified with the laser microdissection-based microproteomic method. These include, in the cyst: *m*/*z* 887.6 corresponding to tubulin alpha; *m*/*z* 1031.8 to vitamin K-dependent protein C; *m*/*z* 1646.9 to Ig kappa chain V–III region NG9, in the cyst wall: *m*/*z* 1004.6 to Ras-related protein Rab-35; *m*/*z* 1212.7 to integrin alpha-M; *m*/*z* 1777 to UBX domain-containing protein 1, in the liver: *m*/*z* 907.5 to aminomethyltransferase, mitochondrial; *m*/*z* 1436.7 to cytochrome P450, 2C8 and *m*/*z* 1493.7 to UDP-glucuronosyltransferase 1–6. The merged image shows the overlaid distribution of three specific peaks (*m*/*z*, 907.5 in green, *m*/*z* 1646.9 in blue and *m*/*z* 1777 in red). The last image at the bottom right corner represents the statistical segmented image, where each color represents a different molecular pattern. (For interpretation of the references to colour in this figure legend, the reader is referred to the web version of this article.)

In the present study, we applied LMD-based LC–MS/MS and IMS to evaluate the proteomic microanatomical context of CE in the human liver. Although these methods are established on both, FFPE and fresh-frozen (fr/fr) tissue samples, we decided to work on FFPE tissue, since it is the standard method to store tissue blocks in pathology institutes. Although frozen samples are easier to be analyzed and imaged as they do not require multiple steps for sample preparation (deparaffination and antigen retrieval), handling and storage of frozen specimens has disadvantages, since proteins are degraded during repeated freeze-thaw cycles and there is a need for expensive logistics [27]. Also, the apparition of ice crystals during the process of freezing may alter subsequent proteomic analyses [28–30]. The development of molecular methods on FFPE tissues for biomarker discovery and diagnosis holds great promise for universalization.

In order to reverse the process of protein crosslinking induced by the fixative, we used heat-induced antigen retrieval (HIAR) [31]. The principle of the method adapted for microproteomics of FFPE tissues was previously explained and proved efficient for biomarker discovery [21]. In our case, HIAR-based workflow for microproteomics of FFPE tissues allowed identifying proteins from various tissue compartments, namely the cyst, the cyst wall and the surrounding liver tissue. The IMS approach, which also relies on HIAR and on-tissue digestion [24], allowed mapping some of the identified peptides through the tissue section.

Several proteomic studies already focused on the study of Eg [12–20]. However, the number of protein sequences from this species is very limited in classically used databases (26 reviewed protein sequences in Uniprot). In this context, we interrogated databanks of proteins sequences from both, Eg and human for the identifications. Among the proteins assigned to human species, it is highly probable that some of these share common sequences with proteins from Eg that were not yet described.

The defense of the host against parasitic infections involves various immunologic and non-immunologic biochemical pathways [17]. We could identify proteins which are players of the host immune response.

Our findings suggested a strong immunoglobulin response within the cyst.

In the cyst wall, processes of antigen presentation are more likely represented. Among others, e.g. HLA class II histocompatibility antigen gamma chain (CD74), Marginal zone B- and B1-cell-specific protein where found in the cyst wall. Further proteins attributed to antigen presentation include HLA class I histocompatibility antigen, Cw-7 alpha chain, HLA class I histocompatibility antigen and A-36 alpha chain. Only one immunoglobulin type was found only in the cyst wall, Ig kappa chain V–III.

While antigens of Eg were present in the cystic as well as in the cyst wall and the liver, immunological processes were mainly located in the cyst and the cyst wall. Besides proteins of immune cells, such of immune processes (e.g. macrophage migration inhibiting factor) were also found in the cyst wall. Additionally, we found ECM proteins in the cyst wall. The glycoprotein Tenascin was identified. This protein is involved in wound healing and inflammation [32].

Finally, the GO revealed proteins of the larval development of the worm in the liver. This might suggest that even after Eg has formed a cyst, the infection is still molecularly visible in the liver itself. This observation might represent a major asset for molecular diagnosis, in the future. Using Eg markers specifically present in the liver would allow the diagnosis from a single liver biopsy.

Proteolytic peptides were then mapped by IMS in the various compartments. This analysis gives an insight of IMS technology for molecular diagnosis. IMS allows the mapping of hundreds of proteolytic peptides directly from a single tissue section. The presence of specific marker peptides in a liver section may inform of an infection by Eg. Segmentation analyses can reveal different molecular clusters within tissue sections. In our case, the segmentation of the IMS dataset was performed without taking into account the outer part of the tissue. Areas of coagulated tissue due to the surgical process could indeed clearly be distinguished. Each color of the segmentation map represents a different molecular pattern in the tissue. The segmentation map that we obtained suggests molecular heterogeneity from the core of the cyst to the margin of the liver tissue. Those molecular differences might be due to slightly different molecular events in the spatial context of the tissue.

5. Conclusion

This combined approach showed for the first time the association of specific proteins to various compartments, cellular phenotypes, parasitic stages and pathobiochemical as well as immune processes in human liver CE. Since few years, mass spectrometry workflows have raised as potential adjunct methods in molecular pathology [33,34]. In this work, we give an insight of the potential of IMS and LC–MS approaches for future biomarker discovery studies and molecular diagnosis of CE.

Financial support

This work was supported by Proteopath and by the post-doc program of the medical faculty of the University of Heidelberg for M.K.

Conflict of interest

The authors declare that they have no conflict of interest.

Acknowledgments

Lisette Trzpiot and Nancy Rosière (LSM) are gratefully acknowledged for their excellent technical assistance.

Appendix A. Supplementary data

Supplementary data associated with this article can be found, in the online version, at http://dx.doi.org/10.1016/j.molbiopara.2016.12.002.

References

[1] F. Rinaldi, E. Brunetti, A. Neumayr, M. Maestri, S. Goblirsch, F. Tamarozzi, Cystic echinococcosis of the liver: a primer for hepatologists, World J. Hepatol. 6 (5) (2014) 293–305.
[2] T. Pakala, M. Molina, G.Y. Wu, Hepatic echinococcal cysts: a review, J. clin. Transl. Hepatol. 4 (1) (2016) 39–46.
[3] W.H.O.I.W. Group, International classification of ultrasound images in cystic echinococcosis for application in clinical and field epidemiological settings, Acta Trop. 85 (2) (2003) 253–261.
[4] W. Zhang, H. Wen, J. Li, R. Lin, D.P. McManus, Immunology and immunodiagnosis of cystic echinococcosis: an update, Clin. Dev. Immunol. 2012 (2012) 101895.
[5] L. Insabato, G. Marino, F. Fazioli, V. Iacono, M. Mascolo, L. Palombini, Primary intramuscular infestation of Echinococcus granulosus misdiagnosed as a soft tissue tumor: a case report, Acta Cytol. 51 (4) (2007) 631–633.
[6] H.I. Secer, I. Anik, E. Celik, M.K. Daneyemez, E. Gonul, Spinal hydatid cyst mimicking arachnoid cyst on magnetic resonance imaging, J. Spinal Cord Med. 31 (1) (2008) 106–108.
[7] M. Stojkovic, C. Mickan, T.F. Weber, T. Junghanss, Pitfalls in diagnosis and treatment of alveolar echinococcosis: a sentinel case series, BMJ Open Gastroenterol. 2 (1) (2015) e000036.
[8] U. Cobanoglu, F. Sayir, D. Mergan, Diagnostic dilemma: analysis of 11 cases of hydatid disease, Turkiye parazitolojii dergisi/Turkiye Parazitoloji Dernegi = Acta parasitologica Turcica/Turkish Soc. Parasitol. 35 (3) (2011) 164–168.
[9] G. Adas, O. Karatepe, M. Altiok, M. Battal, O. Bender, D. Ozcan, S. Karahan, Diagnostic problems with parasitic and non-parasitic splenic cysts, BMC Surg. 9 (2009) 9.

[10] S. Rostami, S. Shariat Torbaghan, S. Dabiri, Z. Babaei, M. Ali Mohammadi, M. Sharbatkhori, M. Fasihi Harandi, Genetic characterization of Echinococcus granulosus from a large number of formalin-fixed, paraffin-embedded tissue samples of human isolates in Iran, Am. J. Trop. Med. Hyg. 92 (3) (2015) 588–594.
[11] A. Spotin, M.F. Mahami-Oskouei, M. Harandi, A. Baratchian, E. Bordbar, S. Ebrahimi, Genetic variability of Echinococcus granulosus complex in various geographical populations of Iran inferred by mitochondrial DNA sequences, Acta Trop. 165 (2017) 10–16.
[12] G.B. Dos Santos, K.M. Monteiro, E.D. da Silva, M.E. Battistella, H.B. Ferreira, A. Zaha, Excretory/secretory products in the Echinococcus granulosus metacestode: is the intermediate host complacent with infection caused by the larval form of the parasite? Int. J. Parasitol. 46 (13–14) (2016) 843–856.
[13] C. Hidalgo, M.P. Garcia, C. Stoore, J.P. Ramirez, K.M. Monteiro, U. Hellman, A. Zaha, H.B. Ferreira, N. Galanti, E. Landerer, R. Paredes, Proteomics analysis of Echinococcus granulosus protoscolex stage, Vet. Parasitol. 218 (2016) 43–45.
[14] K.R. Lorenzatto, K. Kim, I. Ntai, G.P. Paludo, J. Camargo de Lima, P.M. Thomas, N.L. Kelleher, H.B. Ferreira, Top down proteomics reveals mature proteoforms expressed in subcellular fractions of the echinococcus granulosus preadult stage, J. Proteome Res. 14 (11) (2015) 4805–4814.
[15] C.S. Ahn, X. Han, Y.A. Bae, X. Ma, J.T. Kim, H. Cai, H.J. Yang, I. Kang, H. Wang, Y. Kong, Alteration of immunoproteome profile of Echinococcus granulosus hydatid fluid with progression of cystic echinococcosis, Parasites Vectors 8 (2015) 10.
[16] S.J. Cui, L.L. Xu, T. Zhang, M. Xu, J. Yao, C.Y. Fang, Z. Feng, P.Y. Yang, W. Hu, F. Liu, Proteomic characterization of larval and adult developmental stages in Echinococcus granulosus reveals novel insight into host-parasite interactions, J. Proteom. 84 (2013) 158–175.
[17] A. Siracusano, F. Delunardo, A. Teggi, E. Ortona, Host-parasite relationship in cystic echinococcosis: an evolving story, Clin. Dev. Immunol. 2012 (2012) 639362.
[18] A. Aziz, W. Zhang, J. Li, A. Loukas, D.P. McManus, J. Mulvenna, Proteomic characterisation of Echinococcus granulosus hydatid cyst fluid from sheep, cattle and humans, J. Proteom. 74 (9) (2011) 1560–1572.
[19] K.M. Monteiro, M.O. de Carvalho, A. Zaha, H.B. Ferreira, Proteomic analysis of the Echinococcus granulosus metacestode during infection of its intermediate host, Proteomics 10 (10) (2010) 1985–1999.
[20] G. Chemale, A.J. van Rossum, J.R. Jefferies, J. Barrett, P.M. Brophy, H.B. Ferreira, A. Zaha, Proteomic analysis of the larval stage of the parasite Echinococcus granulosus: causative agent of cystic hydatid disease, Proteomics 3 (8) (2003) 1633–1636.
[21] R. Longuespee, D. Alberts, C. Pottier, N. Smargiasso, G. Mazzucchelli, D. Baiwir, M. Kriegsmann, M. Herfs, J. Kriegsmann, P. Delvenne, E. De Pauw, A laser microdissection-based workflow for FFPE tissue microproteomics: important considerations for small sample processing, Methods 104 (2016) 154–162.
[22] M. Kriegsmann, R. Casadonte, J. Kriegsmann, H. Dienemann, P. Schirmacher, J.H. Kobarg, K. Schwamborn, A. Stenzinger, A. Warth, W. Weichert, Reliable entity subtyping in non-small cell lung cancer by MALDI imaging mass spectrometry on formalin-fixed paraffin-embedded tissue specimens, Mol. Cell. Proteom. 15 (10) (2016) 3081–3089.
[23] R. Longuespee, H. Gagnon, C. Boyon, K. Strupat, C. Dauly, O. Kerdraon, A. Ighodaro, A. Desmons, J. Dupuis, M. Wisztorski, D. Vinatier, I. Fournier, R. Day, M. Salzet, Proteomic analyses of serous and endometrioid epithelial ovarian cancers – cases studies – molecular insights of a possible histological etiology of serous ovarian cancer, Proteom. Clin. Appl. 7 (5–6) (2013) 337–354.
[24] R. Casadonte, R.M. Caprioli, Proteomic analysis of formalin-fixed paraffin-embedded tissue by MALDI imaging mass spectrometry, Nat. Protoc. 6 (11) (2011) 1695–1709.
[25] M. Ashburner, C.A. Ball, J.A. Blake, D. Botstein, H. Butler, J.M. Cherry, A.P. Davis, K. Dolinski, S.S. Dwight, J.T. Eppig, M.A. Harris, D.P. Hill, L. Issel-Tarver, A. Kasarskis, S. Lewis, J.C. Matese, J.E. Richardson, M. Ringwald, G.M. Rubin, G. Sherlock, Gene ontology: tool for the unification of biology. The Gene Ontology Consortium, Nat. Genet. 25 (1) (2000) 25–29.
[26] K. Brehm, M. Spiliotis, R. Zavala-Gongora, C. Konrad, M. Frosch, The molecular mechanisms of larval cestode development: first steps into an unknown world, Parasitol. Int. (55 Suppl) (2006) S15–21.
[27] J. Kriegsmann, M. Kriegsmann, R. Casadonte, MALDI TOF imaging mass spectrometry in clinical pathology: a valuable tool for cancer diagnostics (review), Int. J. Oncol. 46 (3) (2015) 893–906.
[28] M. Sjostrom, Ice crystal growth in skeletal muscle fibres, J. Microsc. 105 (1) (1975) 67–80.
[29] A.K. Christensen, Frozen thin sections of fresh tissue for electron microscopy, with a description of pancreas and liver, J. Cell Biol. 51 (3) (1971) 772–804.
[30] T.C. Appleton, A cryostat approach to ultrathin dry frozen sections for electron microscopy: a morphological and x-ray analytical study, J. Microsc. 100 (1) (1974) 49–74.
[31] O.J. Gustafsson, G. Arentz, P. Hoffmann, Proteomic developments in the analysis of formalin-fixed tissue, Biochim. Biophys. Acta 1854 (6) (2015) 559–580.
[32] R. Chiquet-Ehrismann, M. Chiquet, Tenascins: regulation and putative functions during pathological stress, J. Pathol. 200 (4) (2003) 488–499.
[33] R. Longuespee, R. Casadonte, M. Kriegsmann, C. Pottier, G. Picard de Muller, P. Delvenne, J. Kriegsmann, E. De Pauw, MALDI mass spectrometry imaging: a cutting-edge tool for fundamental and clinical histopathology, Proteom. Clin. Appl. 10 (7) (2016) 701–719.
[34] M. Kriegsmann, P. Wandernoth, K. Lisenko, R. Casadonte, R. Longuespée, N. Arens, J. Kriegsmann, Detection of HPV subtypes by mass spectrometry in FFPE tissue specimens: a reliable tool for routine diagnostics, J. Clin. Pathol. (2016), in press.